Iron implantation in gadolinium gallium garnet studied by conversion-electron Mössbauer spectroscopy

1998 J. Phys.: Condens. Matter 10 101

(http://iopscience.iop.org/0953-8984/10/1/012)

J. Phys.: Condens. Matter **10** (1998) 101–110. Printed in the UK PII: S0953-8984(98)87150-6

Iron implantation in gadolinium gallium garnet studied by conversion-electron Mössbauer spectroscopy

I Szűcs†, I Dézsi†§, Cs Fetzer† and G Langouche‡

† MTA-KFKI Research Institute for Particle and Nuclear Physics, H-1525 Budapest, 114 PO Box 49, Hungary

‡ IKS, Katholieke Universiteit Leuven, B-3001 Leuven, Belgium

Received 27 August 1997, in final form 27 October 1997

Abstract. Gadolinium gallium garnet single crystals were implanted with doses of ^{57}Fe ions in the range 8×10^{15}–6×10^{16} atoms cm^{-2}. Depending on the dose, iron with Fe^{2+} or Fe^{3+} charge states was found to have formed after the implantation. After a subsequent annealing in air, the iron oxidized to Fe^{3+}. The Mössbauer and channelling measurements showed lattice recrystallization taking place at 600 °C. After recrystallization, the iron was found to have substituted for gallium ions both at the octahedral and at the tetrahedral positions. The relative concentration of the two types of iron at the two sites shifted towards the equilibrium distribution upon high-temperature annealing.

1. Introduction

Ion implantation is generally used to modify the properties of various materials. Ion-implantation and annealing effects in semiconductors have been intensively studied, but far fewer studies have been devoted to implanted insulators. In the course of our programme which is being pursued with the aim of obtaining more results on insulators, we performed Mössbauer and channelling studies on iron-implanted $Gd_3Ga_5O_{12}$ (GGG) garnet. GGG can be grown in such a way as to provide excellent single-crystalline quality. Garnets were intensively studied in the 1980s with the aim of developing magnetic bubble devices [1–4]. Later on, ion implantation was used for doping garnets with various ions to prepare laser materials [5]. $Y_3Al_5O_{12}$ (YAG) and GGG crystals were implanted with a high dose of iron with the practical aim of trying to make ferromagnetic garnets out of nonmagnetic ones [6–8]. In these experiments, very high ($\geqslant 10^{17}$ atoms cm^{-2}) doses of iron were implanted. Mössbauer effect studies showed magnetic hyperfine-split spectra for GGG. Because of the high local iron concentration, a large fraction of the implanted iron segregated in complex oxide phases. Since until now GGG crystals have only been implanted with high doses of iron, we set out to perform dose-dependent experiments in an endeavour to learn about the local structure, the oxidation state of the iron implanted at various doses and the annealing behaviour of the implanted layers. Therefore, Mössbauer, Rutherford backscattering and channelling studies were carried out on GGG implanted with ^{57}Fe at various doses.

§ Also at: MTA-KFKI Research Institute for Materials Science, Budapest, Hungary.

0953-8984/98/010101+10$19.50

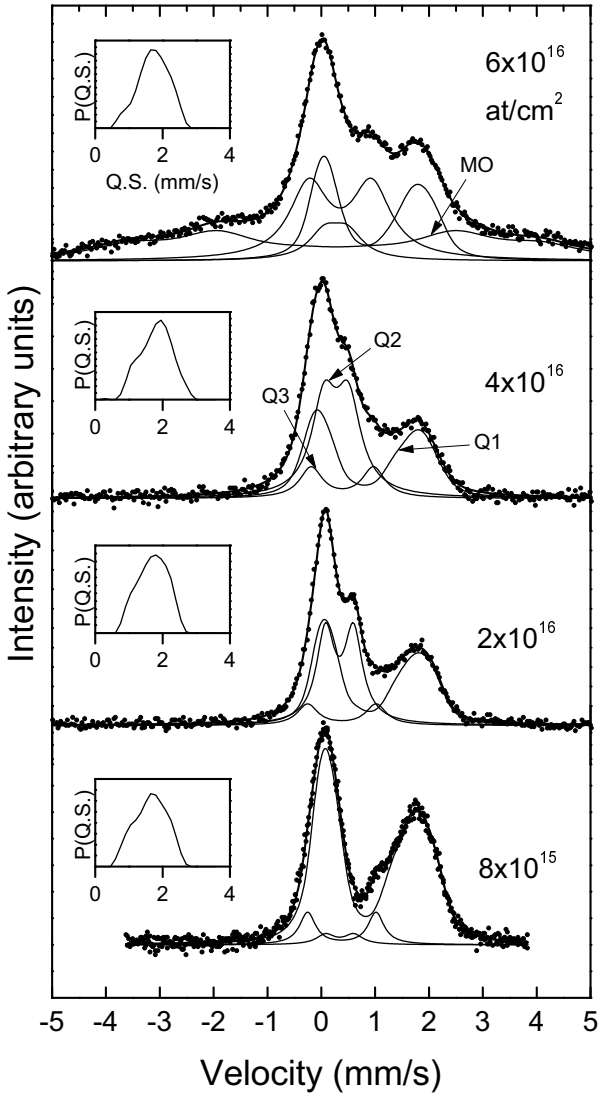

Figure 1. Mössbauer spectra of ^{57}Fe for the as-implanted samples.

2. Experimental details

⟨111⟩ $Gd_3Ga_5O_{12}$ single crystals were implanted with ^{57}Fe at 80 keV at room temperature. The conversion-electron Mössbauer spectra were measured by using a low-background small sized continuous-flow proportional counter. He gas with 4% methane was used in the flow counter. For the measurements at 80 K the counter was placed in a cryostat cooled with liquid nitrogen. The annealing of the samples took place in air. The annealings were performed for ten minutes at each temperature. For the single-line Mössbauer source, 20 mCi ^{57}Co in a Rh matrix was used. The measurements were carried out at room temperature.

Analyses of the Mössbauer spectra were performed by using a program allowing

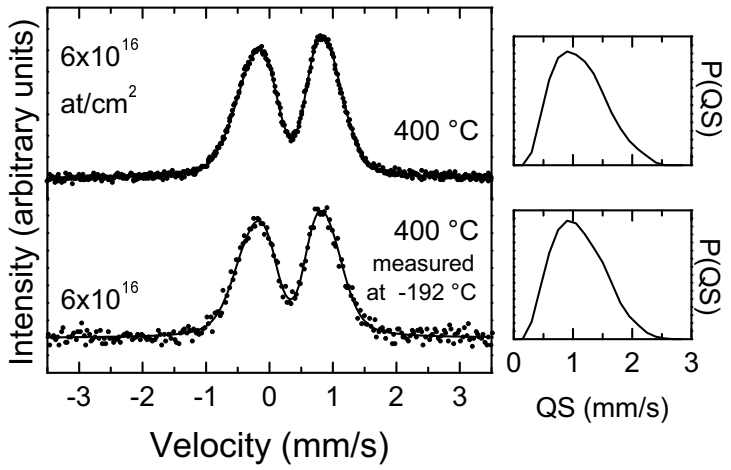

Figure 2. Mössbauer spectra of the sample annealed at 400 °C.

Table 1. Mössbauer parameters of the as-implanted samples. Relative intensities are given as percentages, while the I.S., Q.S. and standard deviation values are given in mm s^{-1}; the magnetic field values (H) are given in teslas. Average values are denoted by $\langle\ \rangle$. The I.S. values are relative to that of α-iron.

Dose	Q1				Q2		
(atoms cm^{-2})	Intensity	⟨I.S.⟩	⟨Q.S.⟩	S.D. Q.S.	Intensity	I.S.	Q.S.
8×10^{15}	86(8)	0.92(2)	1.67(3)	0.50(1)	4(1)	0.35(2)	0.52(2)
2×10^{16}	52(5)	0.92(2)	1.69(3)	0.46(1)	38(4)	0.34(1)	0.52(1)
4×10^{16}	41(4)	0.85(2)	1.76(3)	0.46(2)	44(4)	0.28(1)	0.45(2)
6×10^{16}	26(2)	0.92(2)	1.73(3)	0.45(2)	9(1)	0.27(1)	0.42(2)

Dose	Q3			Sextet		
(atoms cm^{-2})	Intensity	I.S.	Q.S.	Intensity	⟨I.S.⟩	⟨H⟩
8×10^{15}	10(2)	0.38(2)	1.27(2)			
2×10^{16}	10(2)	0.38(2)	1.27(2)			
4×10^{16}	15(2)	0.38(2)	1.16(2)			
6×10^{16}	30(3)	0.35(2)	1.16(2)	35(4)	0.27(3)	23.7(3)

distributions in the hyperfine parameters. Also, fitting of a spectrum having components both with and without a distribution in the parameter values could be performed. In the case of the distribution, the program first calculates theoretical spectra for the various hyperfine interactions, including electric quadrupole interaction. The full static Hamiltonian is used. Setting the isomer shift value to zero and normalizing the spectra to unit area, we obtained a set of parameter points. The cubic spline method was used to calculate a smooth curve going through the points of the set. In order to fit the spectra with a distribution in the parameters, the calculated spectra are read in and corrected for the differences in velocity scale and isomer shifts. The corrected spectra were then fitted to the experimental ones and the fitting procedure gave the relative intensities of the subspectra and the distribution of the parameters. A linear relationship between the isomer shift and the quadrupole-split values of the subspectra was assumed. The isomer shift (I.S.) values are given relative to

Table 2. Mössbauer parameters of samples annealed at 300–500 °C

Implantation dose (atoms cm^{-2})	Annealing temperature (°C)	Quadrupole distribution		
		⟨I.S.⟩ (mm s^{-1})	⟨Q.S.⟩ (mm s^{-1})	S.D. Q.S. (mm s^{-1})
2×10^{16}	300	0.32(1)	1.27(1)	0.46(2)
	500	0.31(2)	1.27(1)	0.48(1)
6×10^{16}	300	0.32(2)	1.10(1)	0.43(1)
	400	0.32(2)	1.11(1)	0.43(1)
	400	0.35(1)*	1.11(1)*	0.43(1)*
	500	0.33(2)	1.13(2)	0.44(2)

* Measured at −193 °C.

that of α-iron.

The Rutherford backscattering and channelling measurements were carried out at the 5 MeV Van de Graaf accelerator of KFKI-RMKI, with the detector placed so as to detect ions scattered through 165°. A liquid-nitrogen-cooled trap was used in order to minimize hydrocarbon deposition. The depth distribution of the atoms was measured by 2 MeV $^4He^+$ channelling along the ⟨111⟩ axis and evaluated by RBX code [9].

3. Results

The Mössbauer spectra of the as-implanted samples are shown in figure 1.

The shapes of the spectra are strongly dose dependent. At least three quadrupole-split spectral components can be distinguished. The spectrum of the sample implanted with the lowest (8×10^{15} atoms cm^{-2}) dose is asymmetric: the resonance emission line on the right-hand side of the spectrum is broader than the line on the left-hand side, indicating a distribution in the hyperfine splitting values. For the spectrum component Q1, a distribution in the isomer shift (I.S.) and quadrupole splitting (Q.S.) values was assumed. Measurements were taken with the sample at different angles relative to the γ-ray incidence to determine whether any orientation of the electric field gradient exists after implantation. The relative intensities of the lines measured at 0° and 54° (the latter is the magic angle, at which the intensity ratio of the two resonance lines of the quadrupole doublet is unity even in the case of orientation of the electric field gradient) relative to the γ-incidence direction were found to be equal within the statistical error. Therefore, the asymmetry does not result from the orientation of the electric field gradient. The asymmetry cannot be explained by the existence of a single-line component at I.S. $\simeq$ 0 mm s^{-1} representing iron in a metallic host as was observed for yttrium aluminium garnet implanted with a very high dose of iron [10]. The formation of metallic iron has not been observed upon implanting iron in oxide crystals at such a low dose value as 8×10^{15} atoms cm^{-2} [11, 12]. Furthermore, at higher dose values the relative intensity of a supposed single-line component would increase at $\simeq$0 mm s^{-1}, contrary to what is observed by us. A reasonable fit could not be obtained by supposing the existence of a single line at $\simeq$0 mm s^{-1} for the spectra implanted with higher doses. Two further spectral components (Q2, Q3) appeared with smaller I.S. and Q.S. values. With increasing dose values the relative intensity of the doublet Q2 first increased, then decreased. The linewidth of these doublet components was in the range 0.39–0.56 mm s^{-1} except for Q2 implanted with the highest dose, giving a value of 0.87 mm s^{-1}. For the sample implanted with 6×10^{16} atoms cm^{-2}, a broad component with an average linewidth

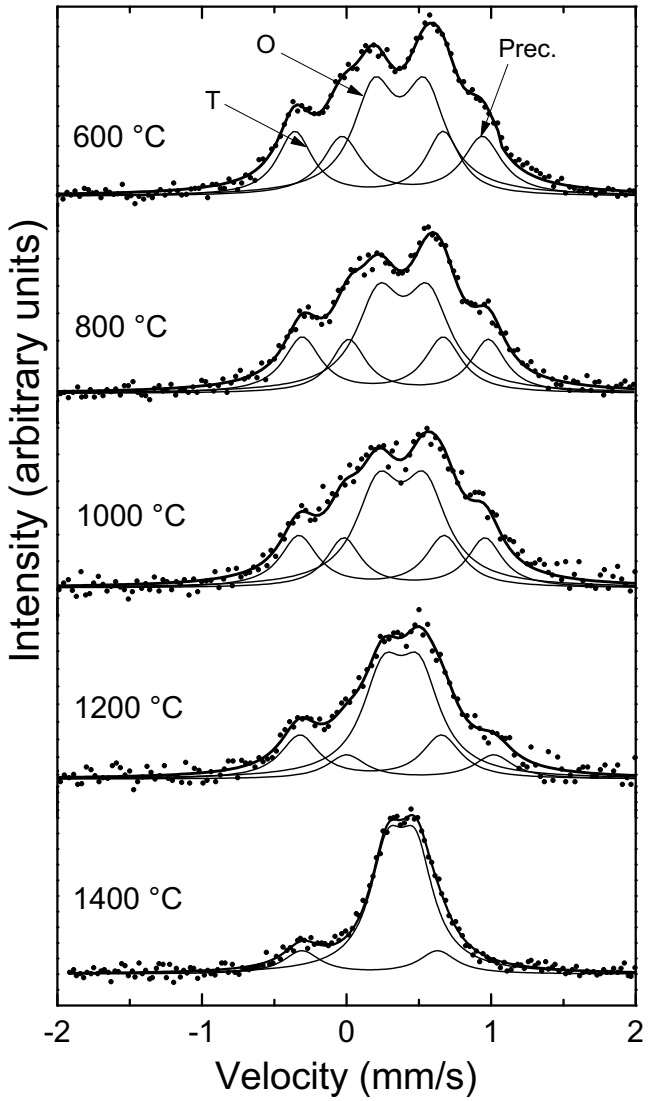

Figure 3. Mössbauer spectra of the samples annealed in air at and above 600 °C. Dose: 2×10^{16} atoms cm^{-2}.

of 1.8(2) mm s^{-1} appeared, indicating magnetic ordering with a distribution of the internal magnetic field value. The parameters of the spectral components for the samples implanted with different doses are compiled in table 1.

Figure 2 shows the spectra obtained after annealing the samples in air from 300 to 500 °C. No change was found in the spectra when annealing was carried out below 300 °C. The spectra show broadened doublets; the relative intensities of the two lines are different. The spectra of the samples implanted with different doses showed the same transformation, and the parameters obtained have close values. If the annealing took place in a vacuum, the spectra of the as-implanted samples did not change for annealing at up to 500 °C, indicating that the oxygen diffused in the implanted layer in air. The spectra could be fitted

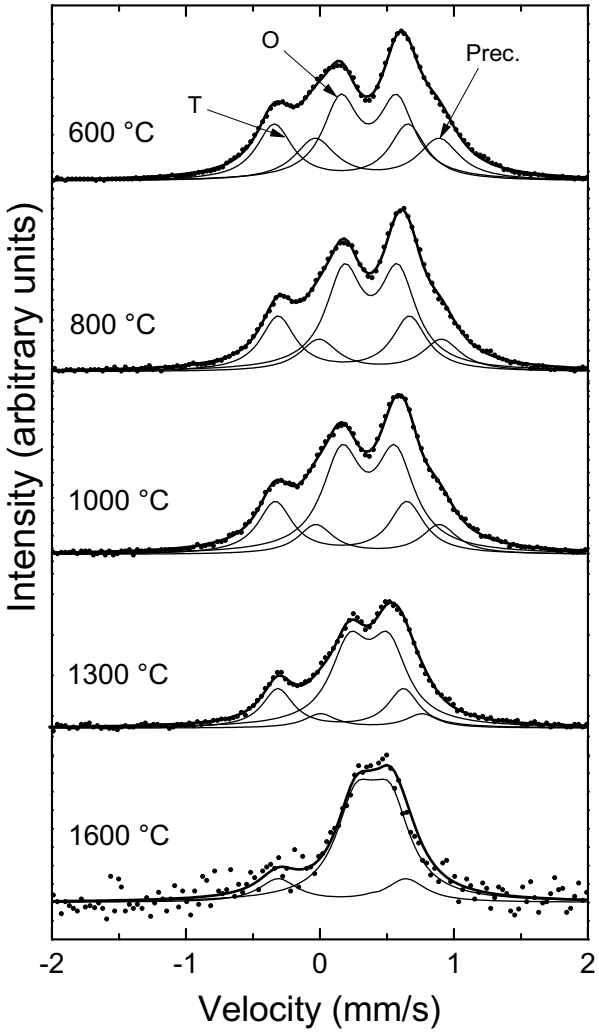

Figure 4. Mössbauer spectra of the samples annealed in air at and above 600 °C. Dose: 6×10^{16} atoms cm^{-2}.

by quadrupole doublets having distributions in their I.S. and Q.S. values. For the sample implanted with 6×10^{16} atoms cm^{-2} the spectrum was also measured at −193 °C, but it was found that the shape had not changed significantly relative to that measured at room temperature. The parameter values are given in table 2.

The spectra changed significantly upon annealing at 600 °C. Also, the Rutherford backscattering spectra of the samples (the spectrum of the sample implanted with a dose of 4×10^{16} atoms cm^{-2} is shown in figure 7—see later) indicated the partial recrystallization of the implanted layer at 600 °C. The spectra of two samples implanted with different doses and annealed at 600 °C and above are shown in figures 3 and 4. The spectra could be fitted by three quadrupole doublets labelled 'O', 'T' and 'Prec.'. The relative intensity, I.S. and Q.S. values are shown in figures 5 and 6. Upon annealing at higher temperatures, the Q.S. values decreased whereas the I.S. values did not change significantly. The total

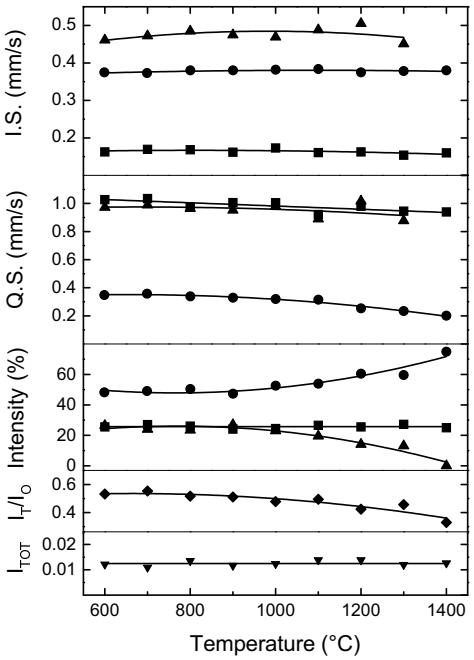

Figure 5. Isomer shift (I.S.) and quadrupole splitting (Q.S.) values, and the relative intensity of the component spectra relating to various iron sites. Full squares: tetrahedral; full circles: octahedral; black upright triangles: segregated iron oxide positions; I_T = tetrahedral fraction; I_O = octahedral fraction. Dose: 2×10^{16} atoms cm^{-2}.

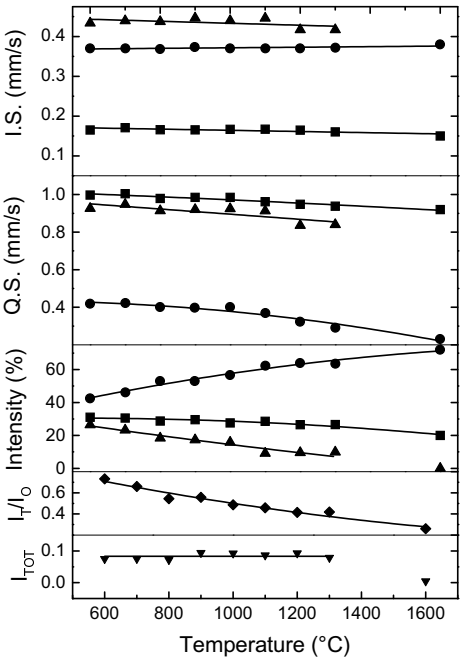

Figure 6. Isomer shift (I.S.) and quadrupole splitting (Q.S.) values, and the relative intensity of the component spectra relating to various iron sites. Full squares: tetrahedral; full circles: octahedral; black upright triangles: segregated iron oxide positions; I_T = tetrahedral fraction; I_O = octahedral fraction. Dose: 6×10^{16} atoms cm^{-2}.

intensity values did not change, except upon annealing at 1600 °C, probably because of the diffusion of iron deeper into the bulk. The relative intensity of the component labelled 'Prec.' and attributed to iron in precipitated oxide decreased gradually upon annealing, and reached the value zero upon annealing at 1400 °C. The ratio of the intensities of the two spectral components T and O (I_T/I_O in figures 5 and 6) decreased upon going to higher annealing temperatures.

The Rutherford backscattering spectrum of the as-implanted sample showed partial disorder (see figure 7). The disorder decreased only upon annealing at 600 °C. The spectra indicated the gradual recrystallization of the implanted layer. At higher temperatures the shape of the RBS spectra changed and became close to the shape of the virgin sample, but the backscattered intensity did not actually reach the value for the virgin sample. No further improvement in the recrystallization of the implanted layer could be observed above 1100 °C in the case of the samples annealed in air.

4. Discussion

The I.S. and Q.S. values of the spectral components of the as-implanted samples indicate that the iron is in Fe^{2+} and in Fe^{3+} high-spin states after implantation. The relative fraction of the iron in the different states is dose dependent. Most of the iron is in the Fe^{2+} state (component Q1) for the low dose values, like that observed in other implanted oxide

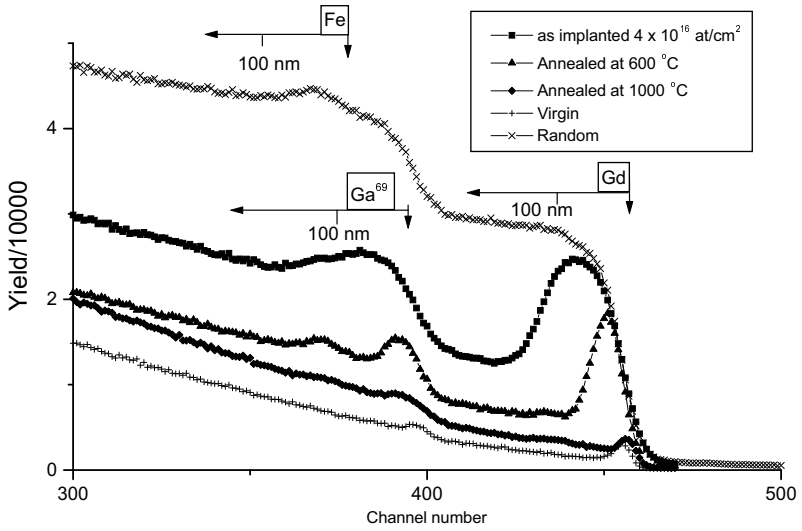

Figure 7. Aligned and random RBS spectra of the sample implanted with 4×10^{16} atoms cm^{-2} of ^{57}Fe.

crystals [11, 12]. The absorption line is broad, indicating a distribution in the parameter values. The distribution may result from the disordering in the neighbourhood. The standard deviation of the distribution of the I.S. value is 0.06(2) mm s^{-1}, a considerably lower value than the 0.45(1) mm s^{-1} S.D. Q.S. value, thereby indicating that the broadening is caused mainly by the topological effect of the surrounding atoms. Two other spectral components (Q2, Q3) appeared with I.S. = 0.35(2), Q.S. = 0.52(2) mm s^{-1} and I.S. = 0.38(2), Q.S. = 1.27 mm s^{-1} values, indicating Fe^{3+} ions. Their relative fraction was increased upon going to higher dose values. The intensity of component Q3 had its maximum value at the highest dose; it is assumed that this component and the partially ordered magnetically split component represent the iron atoms in a highly disordered surrounding.

When the as-implanted samples were annealed in air at 300 °C, the Fe^{2+} component oxidized to Fe^{3+}, indicating the diffusion of oxygen into the implanted layer. The ⟨I.S.⟩ and ⟨Q.S.⟩ values are close to the values for the Q3 component of the as-implanted samples, suggesting again that these spectra relate to iron atoms in a highly disordered surrounding. There was no evidence of magnetic ordering at 80 K; this suggests the presence of separated Fe^{3+} ions or oxide clusters of very small size. In comparison, at 1×10^{17} atoms cm^{-2} implantation dose, segregated magnetically ordered α-Fe_2O_3 formed upon oxidation in YAG [10].

Upon annealing the samples at 600 °C, the spectra (shown in figures 3 and 4) become transformed. Three quadrupole-split spectral components with narrow linewidth values could be recognized. This change indicates recrystallization of the implanted layer. The cubic structure of garnets is built up of octahedra and tetrahedra in which each octahedron is joined to six others through vortex-sharing tetrahedra. Larger ions (Gd^{3+} in our case) occupy positions of eightfold coordination. The Ga^{3+} ions in GGG populate the octahedral (a) and tetrahedral (d) positions in a ratio of 2 to 3. Trivalent ions may substitute for each other at both of these positions, as was observed for YIG and YAlG structures [13–15]. X-ray diffraction studies of various garnets of composition $R_3M_5O_{12}$ showed that the a and the d sites are trigonally and tetragonally distorted, respectively [16]. Also, the trigonal

distortion decreases with the lattice constant. The Mössbauer spectral components of Fe^{3+} ions at the a and d positions were identified. For YIG, the components with I.S. = 0.35, Q.S. = 0.45 and I.S. = 0.16, Q.S. = 1.0 were respectively attributed to Fe^{3+} at a and d sites. The spectral components corresponding to the a and d sites are quadrupole-split doublets. We are able to identify two components labelled O and T in our spectra (figures 3 and 4) for the samples annealed at 600 °C (with the following parameters: I.S. = 0.37, Q.S. = 0.35 mm s^{-1} and I.S. = 0.16, Q.S. = 1.03 mm s^{-1}) for Fe^{3+} ions at a and d positions. The Q2 component appearing in the as-implanted spectra has similar I.S. and Q.S. values to the octahedral component in the annealed samples. The intensity of the Q2 component was found to be decreased at the highest dose value, at which the greatest degree of disordering takes place. Therefore, it is probable that at lower dose values, a fraction of the implanted atoms have similar atomic surroundings to those of the octahedral lattice positions. The Q.S. values of component O were decreased at higher annealing temperatures. This change may be the result of the increasing degree of substitution of Fe^{3+} ions for Ga^{3+} ions, leading to a decrease in the distortion of the octahedra. A similar decrease was observed in aluminium-substituted YIG [14]. Decreased distortion may also result from the gradually decreasing concentration of the defects in the layer caused by high-temperature annealing. This change may explain the decrease of the Q.S. values for Fe^{3+} at the tetrahedral sites, because decreased tetragonal distortion with a decrease in the lattice constant was not observed. The third component ('Prec.') indicates the formation of a segregated oxide phase. This phase is formed because the trivalent-ion concentration in the implanted volume is above the stoichiometric composition in the implanted layer. The relative intensity of this component gradually decreases on going to higher annealing temperatures, and such a phase is not present in the samples annealed above 1300 °C. The relative intensity of the octahedral component increases simultaneously. The relative fraction of the tetrahedral component is also dependent on the dose and annealing temperature but to a smaller degree than it is for the other components. For the sample implanted with the highest dose, this change is very pronounced.

The relative intensity changes depending on the dose and annealing temperatures indicate changes in the cation distributions at the various lattice sites in the layer. On assuming the same Mössbauer–Lamb factor for the Fe^{3+} ions at the different positions, the relative intensity of the various components represents the number of Fe^{3+} ions in the different positions. At the different doses, for the garnet composition written as $Gd_3Ga_tFe_{5-t}O_{12}$, the average t-values can be estimated. For the depth distribution of the implanted atoms, the TRIM program [17] gives 333 Å longitudinal range and 154 Å straggling (σ). The estimated average numbers of iron atoms per centimetre squared in 2σ-thickness are 5.44×10^{15}, 1.3×10^{16}, 2.7×10^{16} and 4.1×10^{16} atoms cm^{-2} at the different dose values. Using these values, the relative numbers of Fe^{3+} and Ga^{3+} ions and the t-value can be estimated for the different doses. The estimation gives better results for lower doses than for higher ones. The values are 4 and 2.7 for the 2×10^{16} and 6×10^{16} atoms cm^{-2} dose values, respectively. In garnets, the distribution of the cations at the tetrahedral and octahedral lattice sites in thermodynamic equilibrium depends on t and on the chemical potential of the cation species in the sublattices [18]. The t-dependence of the distribution D/A (D = tetrahedral, A = octahedral fraction) was determined for $Y_3Ga_tFe_{5-t}O_{12}$ [13], showing a preference of the Fe population to be at the tetrahedral positions at low t-values. We obtained 0.53 and 0.73 for the D/A values after annealing at 600 °C the samples that were implanted with 2×10^{16} and 6×10^{16} atoms cm^{-2} doses, respectively. Both values are higher than those that were measured for the corresponding t-values (0.46 and 0.63) for the Ga-substituted yttrium iron garnets. The difference may be caused by the fact that the

population of the crystalline site was not in thermal equilibrium during the first annealing treatment. The value 0.53 decreased upon going to higher annealing temperatures to 0.45—close to the value measured for Ga-substituted YIG for $t = 2.8$. The value 0.73 decreased to 0.42 upon higher-temperature annealing. This decrease may also result from the change of the local Fe/Ga ratio because of the migration of ions at high temperatures. The lowest D/A value of 0.26 was measured after annealing the sample at 1600 °C, at which stage the out-diffusion of the iron from the implanted layer became apparent.

5. Conclusions

Fe^{2+} and Fe^{3+} ionic states were formed in $Gd_3Ga_5O_{12}$ upon ^{57}Fe-ion implantation. The relative fractions of these ions and the local structure of Fe^{3+} were found to be dose dependent. On annealing the implanted samples at relatively low temperature in air, the Fe^{2+} ions oxidized to Fe^{3+}. The disordered phase recrystallized at 600 °C, and the Fe^{3+} ions distributed among the octahedral and tetrahedral lattice positions with a preference for the population to be at the octahedral positions, like for other iron-substituted garnets. Some of the fraction of the Fe^{3+} ions were found in a segregated oxide phase. The relative fraction of this phase gradually decreased on going to higher annealing temperatures, and it cannot be detected above 1300 °C. Since the total intensity of the Mössbauer effect did not change over the broad annealing temperature range, from this phase the Fe^{3+} ions must have built up into the octahedral lattice sites during the recrystallization of the implanted layer.

Acknowledgments

The authors are indebted to Drs B Keszei and J Vandlik for the GGG crystals used in this study. This work was supported by OTKA grants No T 14235 and No F 4461.

References

[1] Gérard P 1984 *Thin Solid Films* **114** 1
[2] Hirko R and Ju K 1980 *IEEE Trans. Magn.* **16** 958
[3] Speriosu V S and Wilts C H 1983 *J. Appl. Phys.* **54** 3325
[4] Gérard P, Martin P and Delaye M T 1985 *J. Appl. Phys.* **57** 4058
[5] Field S J, Hanna D C, Large A C, Shepherd D P, Tropper A C, Chandler P J, Townsend P D and Zhang L 1991 *Opt. Commun.* **86** 161
[6] Marest G, Kornilios N, Perez A, Ravel F, Gérard P, Gilles B and Brunel M 1987 *Acta Phys. Pol.* A **72** 329
[7] Marest G, Perez A, Gérard P and Mackowski J M 1986 *Phys. Rev.* B **34** 4831
[8] Marest G, Kornilios N, Perez A, Gérard P, Gilles B and Brunel M 1987 *Hyperfine Interact.* **35** 943
[9] Kótai E 1994 *Nucl. Instrum. Methods* B **85** 588
[10] Marest G, Kornilios N, Perez A and Gérard P 1986 *Hyperfine Interact.* **29** 1249
[11] Dézsi I, Coussement R, Fehér S, Langouche G and Fetzer Cs 1986 *Hyperfine Interact.* **29** 1275
[12] Sawicki J A, Marest G, Cox B and Julian S R 1988 *Nucl. Instrum. Methods* B **32** 79
[13] Czerlinsky E R 1969 *Phys. Status Solidi* **34** 483
[14] Czerlinsky E R and MacMillan R A 1970 *Phys. Status Solidi* **41** 333
[15] Lyubutin I S 1971 *Proc. Conf. on Application of the Mössbauer Effect* (Budapest: Akadémiai Kiadó) p 467
[16] Euler F and Bruce J 1965 *Acta Crystallogr.* **19** 971
[17] Ziegler J F, Biersack J P and Littmark U 1985 *The Stopping and Ranges of Ions in Solids* (New York: Pergamon)
[18] Borghese C 1967 *J. Phys. Chem. Solids* **28** 2225